Journal of Structural Biology 191 (2015) 10–21

Contents lists available at ScienceDirect

Journal of Structural Biology

journal homepage: www.elsevier.com/locate/yjsbi

Structural outline of the detailed mechanism for elongation factor Ts-mediated guanine nucleotide exchange on elongation factor Tu

Søren S. Thirup *, Lan Bich Van, Tine K. Nielsen [1], Charlotte R. Knudsen

Aarhus University, Department of Molecular Biology and Genetics, Center for Structural Biology, DK-8000 Aarhus C, Denmark

ARTICLE INFO

Article history:
Received 15 March 2015
Received in revised form 5 June 2015
Accepted 11 June 2015
Available online 11 June 2015

Keywords:
Guanine nucleotide exchange
Elongation factor Tu
Elongation factor Ts
G–GEF complex
Crystal structure

ABSTRACT

Translation elongation factor EF-Tu belongs to the superfamily of guanine-nucleotide binding proteins, which play key cellular roles as regulatory switches. All G-proteins require activation via exchange of GDP for GTP to carry out their respective tasks. Often, guanine-nucleotide exchange factors are essential to this process. During translation, EF-Tu:GTP transports aminoacylated tRNA to the ribosome. GTP is hydrolyzed during this process, and subsequent reactivation of EF-Tu is catalyzed by EF-Ts. The reaction path of guanine-nucleotide exchange is structurally poorly defined for EF-Tu and EF-Ts. We have determined the crystal structures of the following reaction intermediates: two structures of EF-Tu:GDP:EF-Ts (2.2 and 1.8 Å resolution), EF-Tu:PO_4:EF-Ts (1.9 Å resolution), EF-Tu:GDPNP:EF-Ts (2.2 Å resolution) and EF-Tu:GDPNP:pulvomycin:Mg^{2+}:EF-Ts (3.5 Å resolution). These structures provide snapshots throughout the entire exchange reaction and suggest a mechanism for the release of EF-Tu in its GTP conformation. An inferred sequence of events during the exchange reaction is presented.

1. Introduction

G-binding proteins are molecular switches that alternate between an active, GTP-bound conformation and an inactive GDP-bound conformation for a regulatory purpose. The exchange of GTP for GDP is the key event in activation of the G-binding proteins. Guanine-nucleotide exchange factors (GEFs) have been identified for most classes of the G-binding proteins and the exchange reaction is believed to proceed through a common set of intermediate states identified in biochemical studies (Guo et al., 2005). The inactive form of the G-binding protein binds its cognate GEF upon formation of a labile ternary complex. GDP is expelled from this complex, which converts into a stable, binary complex. Finally, GTP rebinding takes place via formation of a second, unstable ternary complex from which the GEF is released.

The G-binding protein elongation factor Tu (EF-Tu) binds aminoacyl-tRNA (aa-tRNA) in its GTP-bound state. The GTP is hydrolyzed upon proper binding of aa-tRNA to the A site of the programmed ribosome and EF-Tu:GDP is released and subsequently returned to its active state by elongation factor Ts (EF-Ts), the GEF for EF-Tu. EF-Ts accelerates the rate of nucleotide exchange on EF-Tu by nearly 5 orders of magnitude (Gromadski et al., 2002). The functional cycle of EF-Tu is inhibited by a number of antibiotics (Anborgh et al., 2004; Parmeggiani and Nissen, 2006) including pulvomycin, which prevents formation of the EF-Tu:GTP:aa-tRNA complex and also stabilizes the interaction of EF-Tu with EF-Ts (Anborgh et al., 2004). *In vivo*, the concentration of GTP is approximately 10-times higher than that of GDP, which for most G-binding proteins is sufficient to ensure that the active, GTP-bound conformation is attained after completion of the exchange reaction. In the case of EF-Tu, however, the affinity for GDP is approximately 100 times higher than the affinity for GTP (Gromadski et al., 2002), but subsequent binding of aa-tRNA drives the equilibrium towards formation of the active conformation.

EF-Tu is a three-domain protein of which the N-terminal domain, the G-domain, comprises the nucleotide-binding site that involves five loops, G-1 to G-5 (Bourne et al., 1991). G-1, also referred to as the phosphate-binding loop or the P-loop, has the consensus sequence (A/G)X_4GK(S/T) (single letter amino acid code, where X is any amino acid) (G18HVDHGKT25 in *Escherichia coli* EF-Tu, where the numbers refer to the positions in the primary sequence) and is mainly involved in binding the phosphates. G-2, also called switch 1, has the consensus sequence D$(X)_n$T (D50$(X)_{10}$T61 in *E. coli* EF-Tu) and interacts with the γ-phosphate. G-3 has the consensus sequence motif DXXG (D80CPG83 in *E. coli* EF-Tu), where the aspartate together with T25 of G-1 and the phosphates of the nucleotide coordinate a Mg^{2+} ion essential for nucleotide binding. The term switch 2 refers

* Corresponding author.
E-mail address: sth@mbg.au.dk (S.S. Thirup).
[1] Present address: CMC Biologics, Vandtaarnsvej 83B, DK 2860 Soeborg, Denmark.

http://dx.doi.org/10.1016/j.jsb.2015.06.011
1047-8477/

to G-3 and the following helix B. G-4 and G-5 are conferring specificity for the guanine base. G-4 has the consensus sequence NKXD (N135KCD139 in *E. coli* EF-Tu), while G-5 is characterized by the motif SA(K/L) (S173AL175 in *E. coli* EF-Tu).

The general G-protein undergoes a structural change in the switch 1 and 2 regions upon replacement of GDP by GTP. In EF-Tu, this change progresses into an approximately 90° rotation of the G-domain with respect to the two other domains of EF-Tu (Berchtold et al., 1993; Kjeldgaard et al., 1993) thereby forming the binding site for aa-tRNA (Nissen et al., 1995). While all three domains of EF-Tu interact with aa-tRNA, the binding pocket responsible for discriminating between charged and uncharged tRNA is formed by residues of domain 2 only (Nissen et al., 1995).

Structures of EF-Tu:EF-Ts (TT) complexes from *E. coli* (Kawashima et al., 1996b), *Thermus thermophilus* (Wang et al., 1997) and bovine mitochondria (Jeppesen et al., 2005) have been determined without any ligands. *E. coli* EF-Ts is composed of four domains: the N-terminal domain (residues 1–54), subdomain N (residues 55–140), subdomain C (residues 141–179 and 229–263) and the coiled-coil domain (residues 180–228 comprising helices 9, 10 and 11) as well as a C-terminal extension (residues 264–282). The *E. coli* EF-Tu:EF-Ts structure shows that EF-Ts interacts with EF-Tu at three distinct sites: the N-terminal domain of EF-Ts binds to EF-Tu helix D close to the guanine-binding pocket, subdomain N of EF-Ts binds close to the P-loop and the switch 2 region of EF-Tu and finally subdomain C of EF-Ts binds to domain 3 of EF-Tu. The C-terminal extension of *E. coli* EF-Ts, which is not found in neither *T. thermophilus* nor bovine mitochondrial EF-Ts, additionally binds to EF-Tu at the position which is otherwise occupied by helix A′ of the switch 1 region. Apart from this difference, the interactions between EF-Tu and EF-Ts found in the *T. thermophilus* and bovine mitochondrial structures are very similar to those described for the complex from *E. coli*.

Based on the abovementioned EF-Tu:EF-Ts structures, it was suggested that the release of nucleotide is accomplished by the insertion of sF81 of the conserved TDFV motif of EF-Ts between uH84 and uH118 situated in helices B and C of EF-Tu, respectively (the prefixes "u" and "s" designate residues from EF-Tu and EF-Ts, respectively). Thereby a structural rearrangement is initiated causing a movement of uD80 away from the Mg^{2+} ion, which is released. Removal of the Mg^{2+} ion alone stimulates the rate of GDP dissociation by a factor of 150–300 (Gromadski et al., 2002). The insertion of sF81 also results in a movement of side chains of helix C and, as these are interacting with uH19 and uD21, causes a flip of peptide uV20. This, in turn, affects the position of the side chain of uD21, which becomes stabilized by interaction with sK51. The rearrangements in the P-loop disrupt the binding of the β-phosphate of the guanine nucleotide. Binding of the guanine ring is destabilized by the retraction of uD138 of the NKXD motif due to movement of helix D (Kawashima et al., 1996b).

The effects of mutating single amino acids predicted to be crucial during exchange based on the structure of the EF-Tu:EF-Ts complex were found to be relatively small (Zhang et al., 1996; Dahl et al., 2006; Schummer et al., 2007; Wieden et al., 2002). This indicates that the reaction pathway is more complex and/or that the EF-Tu:EF-Ts structure is unsuitable for delineating the mechanism of guanine-nucleotide exchange, which proceed via a number of intermediary complexes of lower stability. In the case of EF-Tu, the existence of these complexes have been proven by pre-steady state kinetic analysis (Gromadski et al., 2002), but their inherent instability have so far excluded them from X-ray crystallographic analysis. Furthermore, it has recently been shown that the presence of aa-tRNA also affects the rates of transition between the intermediary states of the nucleotide exchange and that quaternary complexes composed of EF-Tu, EF-Ts, aa-tRNA and nucleotide may also exist (Burnett et al., 2014; Burnett et al., 2013). Only few structural studies of intermediary states of G-binding proteins during guanine-nucleotide exchange have been reported, including structures of the yeast homolog of EF-Tu, eEF1A, and a catalytic fragment of its GEF eEF1Bα (Andersen et al., 2001), Arf1 and its GEF Sec7 (Renault et al., 2003), Rop and the catalytic PRONE domain of its GEF RopGEF8 (Thomas et al., 2007), Cdc42 and DOCK9 (Yang et al., 2009), ARA7 and its GEF VPS9a (Uejima et al., 2010) and Rab8·Rabin8 complexes (Guo et al., 2013).

Here we present an extensive set of crystal structures of complexes between EF-Tu and EF-Ts representing discrete steps along the guanine-nucleotide exchange pathway, including the structures of EF-Tu:GDPNP:pulvomycin:Mg^{2+}:EF-Ts (TTTPuM), EF-Tu:PO_4:EF-Ts (TTP), two structures of EF-Tu:GDP:EF-Ts (TTDPa and b) and EF-Tu:GDPNP:EF-Ts (TTTP). Analysis of these structural data along with previously determined structures (Kawashima et al., 1996b; Kjeldgaard et al., 1993; Song et al., 1999) allows a detailed outline of the mechanism for guanine-nucleotide exchange supported by existing biochemical studies.

2. Materials and methods

Detailed experimental procedures for all techniques used are provided in the section on Experimental procedures of the Supplementary Material.

EF-Tu and EF-Ts were expressed and purified as glutathione-S-transferase fusion proteins essentially as previously described (Bogestrand et al., 1995) (Knudsen et al., 1992). Crystals formed in sitting drops within three days, grew to their final size within a week, and were then dehydrated and cryoprotected (Table S1) prior to data collection at 100 K.

For phase determination by molecular replacement of the TTP structure, two search models were constructed based on the structure of *Thermus aquaticus* EF-Tu:GDP (Polekhina et al., 1996), i.e. domain 1 of EF-Tu constituted one model and domains 2 and 3 together constituted the other model. After refinement of TTP, this structure was used as the search model using either the full complex or individual molecules in MR for phasing of the other datasets. Finally, the structures were subjected to alternating rounds of model building and refinement (see Table 1). The structures are deposited in the Protein DataBank (PDB): TTP – 4PC1; TTDPa – 4PC2; TTDPb – 4PC3; TTTP – 4PC6; TTTPuM – 4PC7.

3. Results

3.1. Crystallization and structure determination

TTP, TTDP and TTTP were crystallized under conditions (Table S1) very similar to the previously reported conditions for *E. coli* EF-Tu:EF-Ts (Kawashima et al., 1996a; Yoder et al., 1985) and was found to belong to the same space group, also with two molecules pr asymmetric unit, and with similar cell dimensions (Table 1).

It was essential that purification of the two components and formation of the complex were done within a week without intermittent freezing of protein solutions to obtain crystals diffracting to high resolution after dehydration.

Crystals with GDP could be obtained both in the absence (TTDPa) and presence of Mg^{2+} ions (TTDPb). In general, however, crystals grown in the presence of Mg^{2+} and nucleotide diffracted only to 5 Å resolution, but could be converted to high resolution diffracting crystals, when dehydrated in a solution containing citrate. Hence, structures determined from these dehydrated crystals do not show any Mg^{2+} ions. Crystals grown from PEG6K (Table S1) have two EF-Tu:EF-Ts complexes in the asymmetric unit designated A and B, e.g. TTDPaA denotes complex A of crystal TTDPa. Furthermore,

Table 1
Data collection and refinement statistics.

Data collection	TTP	TTDPa	TTDPb	TTTP	TTTPuM
Beam line	SRS-Daresbury BL9.5	Maxlab Lund BL711	Maxlab Lund BL711	Elettra Trieste XRD	Maxlab Lund BL711
Wavelength (Å)	0.9215	0.944	1.033	1.2	1.033
Detector	MAR 300	MARCCD	MARCCD	MARCCD	MARCCD
Data processing	DENZO	DENZO	XDS	XDS	XDS
Resolution range (Å) (outershell)	68.8–1.95 (2.0–1.95)	35.0–2.2 (2.28–2.20)	58.9–1.84 (1.95–1.84)	29.5–2.2 (2.28–2.20)	29.5–3.6 (3.8–3.6)
R-merge %	9.1 (65.8)	4.4 (25.2)	5.2 (36.9)	10.3 (44.0)	10.8 (42.4)
I/sig(*I*)	11.6 (1.8)	18.1 (4.2)	16.3 (3.9)	13.8 (3.4)	10.7(3.3)
Completeness %	96.8 (97.2)	97.8 (85.3)	98.5 (98.2)	99.5 (98.5)	99.3 (99.9)
Multiplicity	2.7 (2.6)	5.0 (2.2)	6.5 (4.9)	7.7 (4.4)	3.5 (3.5)
Refinement					
Space group	$P\,2_12_12_1$	$P\,2_12_12_1$	$P\,2_12_12_1$	$P\,2_12_12_1$	$P\,3_221$
Unit cell (Å)					
a	73.5	73.9	74.0	74.0	122.8
b	109.8	108.5	108.9	107.5	122.8
c	195.0	193.8	194.8	193.3	173.3
Wilson *B*-factor	21.32	29.21	28.93	35.34	110.58
R-work/*R*-free	0.174/0.208	0.165/0.213	0.159/0.199	0.171/0.223	0.255/0.283
Number of atoms	11,325	10,715	11,293	10,390	4889
Macromolecules	9885	9933	10,021	9802	4795
Ligands	38	73	114	120	93
Water	1402	709	1158	468	1
Protein residues	1284	1301	1295	1286	628
RMS (bonds) (Å)	0.013	0.010	0.012	0.004	0.002
RMS (angles) (°)	1.35	1.17	1.30	0.81	0.52
Ramachandran favored (%)	98	98	99	98	84
Ramachandran outliers (%)	0.16	0.078	0.23	0.00	2.90
Average *B*-factor	32.00	39.00	45.60	47.50	148.10
Macromolecules	31.60	39.10	45.40	47.80	148.4
Ligands	29.90	45.80	60.10	55.90	131.90
Solvent	35.00	37.20	45.90	41.10	100.70

alternate conformations were observed in some structures, which are distinguished by an additional letter, e.g. TTDPbAB is the alternate conformation B of complex A of crystal TTDPb.

TTTP crystals were obtained from a solution containing pulvomycin and GDPNP, but could also be obtained from a solution without pulvomycin. However, the data collected from crystals grown in the presence of pulvomycin extended to a significantly higher resolution, but pulvomycin itself was not observed in the electron density.

TTTPuM crystals were grown in the presence of Mg^{2+}, GDPNP and pulvomycin using ammonium sulfate as the precipitant. The presence of Mg^{2+} was found to be essential for crystal formation in this case.

Data quality, refinement statistics, and model quality indicators are summarized in Table 1.

The general domain orientation in the four crystal structures TTP, TTDPa, TTDPb and TTTP is the same with a root mean square deviation of Cα atoms of any pair of structures less than 0.56 Å (Fig. 1A). Specifically, all contact interfaces are preserved including the contact between the TDFV motif of EF-Ts and domain I of EF-Tu. In contrast to this, a major conformational change towards the EF-Tu:GTP conformation is observed in the structure of the complex containing GDPNP, Mg^{2+} and pulvomycin (TTTPuM) (Fig. 1B). In the following, the structural changes observed upon ligand binding and the new interfaces formed as a result of the major conformational change are described in detail.

3.2. Structures of EF-Tu:GDP:EF-Ts (TTDPaA, TTDPaB, TTDPbA, TTDPbB)

In total, four structures containing GDP were determined from two crystals denoted TTDPa and TTDPb, each with two complexes in the asymmetric unit. Differences in crystallization, soaking and cryo-protection conditions for the two crystals (Table S1) gave rise to significant differences in the nucleotide-binding site even between the two complexes of the asymmetric unit in the same crystal (Fig. 2A and B). Such differences in the same crystal were distinguished by the suffix A or B. In some cases, the electron density of the nucleotide-binding pocket indicated the existence of alternate conformations, which were modeled and denoted with an additional suffix A or B where relevant.

In the P-loop of TTDPa, the phosphates of GDP and the peptide of uV20 occupy nearly the same positions as in EF-Tu:Mg^{2+}:GDP. In contrast, the side chains of uH19 and uH22 are pushed towards the base side of the nucleotide-binding pocket as seen in the EF-Tu:EF-Ts structure. The position of uH22 is stabilized by hydrogen bonding to the side chain of uD109 as in EF-Tu:Mg^{2+}:GDP (Fig. 2A). uD109 itself is also moved towards the base side due to the interaction between sR12 and the main chain of both uD109 and uP111 (Fig. S1A). The amino group of uK24, which forms a salt bridge with the β-phosphate in EF-Tu:Mg^{2+}:GDP is still doing so in TTDPaB, while in TTDPaA it is pointing towards uD80 as previously observed in the ligand-free EF-Tu:EF-Ts complex. However, uD80 assumes two alternate conformations in TTDPaB, one of them similar to the conformation observed in TTDPaA, while the other is pointing away from uK24 (Figs. 2A and S3B). The position of the side chain of uD21 in TTDPaA is not well defined in the electron density even though it is within hydrogen bonding distance of sK51, while in TTDPaB it is well defined in a position pointing away from sK51. Compared to EF-Tu:Mg^{2+}:GDP, the interaction with the guanine ring is destabilized by a small increase in the distance to the side chain of uD138.

The electron density observed in the structure of TTDPbA did not show the distinct features of the two phosphates of GDP and

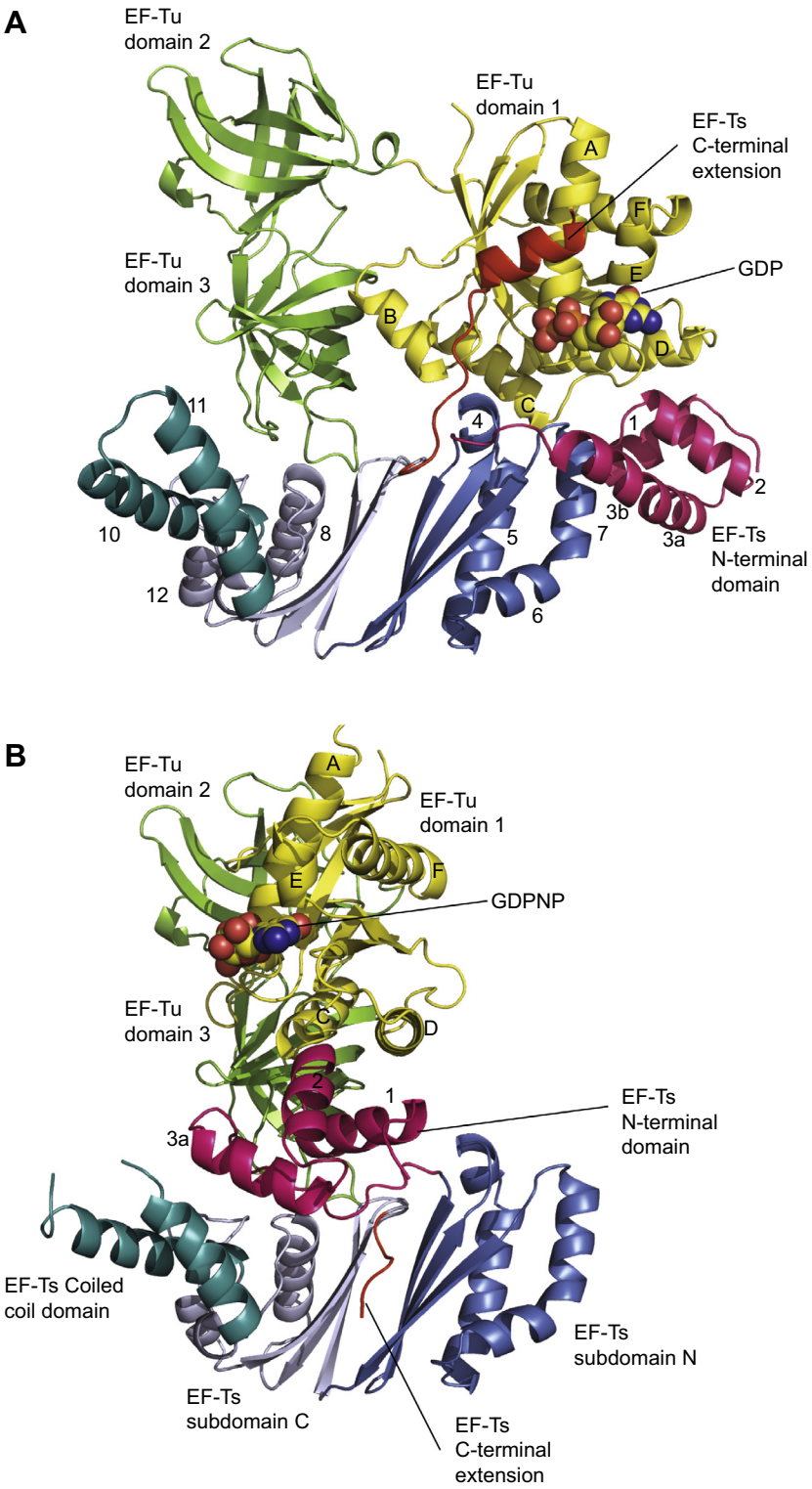

Fig. 1. Cartoon representations of the EF-Tu:EF-Ts complexes. The following color coding applies to all panels: Magenta – EF-Ts N-terminal domain; shades of blue – EF-Ts core domain comprising subdomains N and C; cyan – EF-Ts coiled-coil helices; orange – EF-Ts C-terminal extension; yellow – EF-Tu domain 1; green – EF-Tu domains 2 and 3. The orientations of the complexes in panels A and B are identical for EF-Tu domains 2 and 3 and the EF-Ts core domain. (A) The structure of TTDPa is shown representing the structures of complexes with phosphate (TTP), GDP (TTDP) and GDPNP (TTTP) as they all have the same overall domain orientation. The bound GDP is shown in CPK representation. Helices in domain 1 of EF-Tu are labeled with roman capitals A–F and helices in EF-Ts with numbers 1–13. (B) The structure of TTTPuM. The bound GDPNP is shown in CPK representation. Helices of EF-Tu are labeled with roman capitals A–F and the three helices of the N-terminal domain of EF-Ts are labeled with numbers 1–3. For a superposition of the two conformations see Fig. S1.

furthermore the density suggested that the peptide of uD21 was flipped to the conformation observed in EF-Tu:EF-Ts (Figs. 2B, C and S2C). Hence, the density was modeled as two alternate conformations of the P-loop and correspondingly two alternate positions of GDP. These structures are denoted TTDPbAA and TTDPbAB. In the final refinement, the occupancy of the two

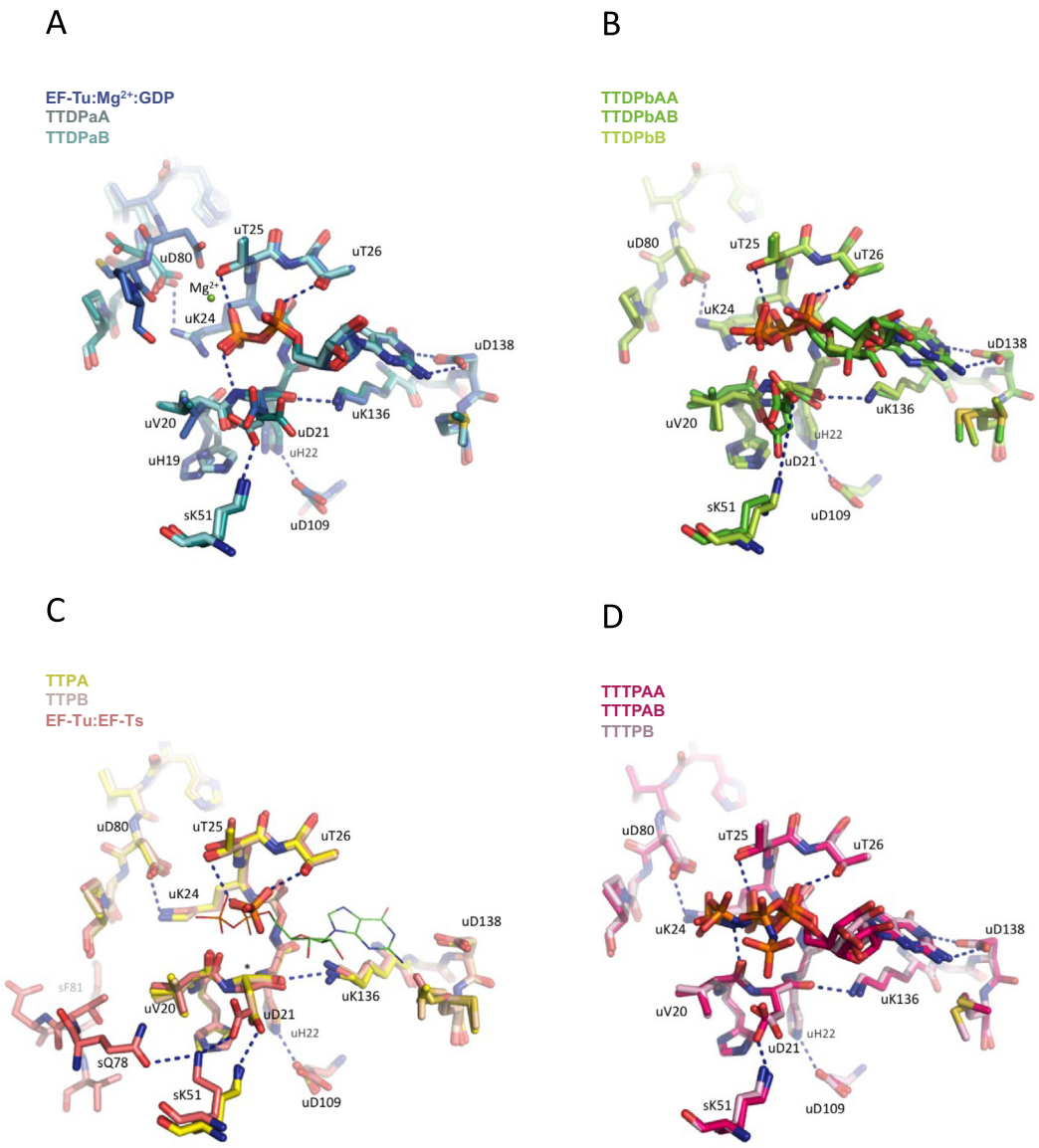

Fig. 2. Structural changes in the nucleotide-binding pocket. A selection of structures specified in the upperleft corners of each panel are superimposed and relevant interactions are indicated by dashed lines. The coloring of the carbon atoms in each panel is given in the list of structures in the upperleft corners. Other atoms are colored as follows: oxygens – red, nitrogens – blue, sulfurs – yellow, phosphate – orange, Magnesium – green. (A) Comparison of EF-Tu:Mg^{2+}:GDP, TTDPaA and TTDPaB. (B) Comparison of TDPbAA, TTDPbAB (alternate conformations of the P-loop and GDP) and TTDPbB. (C) Comparison of TTP, and EF-Tu:EF-Ts. For completeness both TTPA and TTPB are shown although they are nearly identical. For reference, GDP of TTDPcAB is shown as lines. The Cα position of uD21 is indicated by an asterisk. (D) Comparison of TTTPAA, TTTPAB (alternate conformations of GDPNP) and TTTPB. See also Figs. S2 and S3.

alternate P-loop conformations refined to 0.38 and 0.62 for TTDPbAA and TTDPbAB, respectively. Correspondingly, the occupancies of the two alternate GDP conformations refined to 0.37 and 0.43 suggesting a partially empty binding site.

The GDP assumes the same location in the nucleotide binding site in TTDPbB as in TTDPa, but again we observe conformational flexibility for uK24 and uD21; uK24 is modeled as two alternate conformations and the electron density for the side chain of uD21 is weak (Figs. 2B and S2B).

One of the alternate positions of GDP (TTDPbAA) is similar to the position observed in complex TTDPbB, whereas the other position (TTDPbAB) shows a shift of the α-phosphate by 1.3 Å away from the guanine side of the binding pocket. Also the ribose shifts position and there is a change in the torsion angle of the Pα–O5′ and the O5′–C5′ bonds. As a consequence of these movements, the guanine ring is moving out of the binding pocket significantly increasing the distance of the guanine ring to uD138 (Fig. 2B).

3.3. The structure of EF-Tu:PO_4:EF-Ts (TTP)

In the two nearly identical TTP complexes, the phosphate ions are found in the P-loop at a position in between the α and β phosphates of EF-Tu:Mg^{2+}:GDP very close to the position of the α phosphate observed in TTDPbAB (Fig. 2C). The source of the phosphate ion is unknown, but most likely originates from insufficient removal of GDP during formation of the complex. No additional electron density was observed to suggest the location of the remaining part of the GDP (Fig. S3E and F).

The carbonyl group of uV20 has flipped as it is in TTDPbAB and in EF-Tu:EF-Ts. This conformation is stabilized by the formation of a salt bridge between uD21 and sK51 as seen in EF-Tu:EF-Ts. Yet, the salt bridge is slightly longer in TTP due to the presence of the phosphate, which contracts the P-loop thereby moving the Cα of uD21 0.6 Å closer to the phosphate. Also the side chain conformations of both uD21 and sK51 differ between EF-Tu:EF-Ts and TTP.

When the phosphate is released, uD21 moves closer to sK51 and forces the α-amino group towards sQ78 to form a hydrogen bond. This residue is conserved as either a glutamate or glutamine and is located just prior to the conserved TDFV motif of EF-Ts. Furthermore, the conformation of the P-loop in the TTP structure is stabilized by a hydrogen bond between uH22 and uD109, which is absent in EF-Tu:EF-Ts. In the guanine base pocket, the distance between the carbonyl of uD21 and uK136 is slightly increased as compared to TTDPa, and the side chain of uD138 is retracted by more than 1 Å (Fig. 2A and C).

3.4. Structure of the EF-Tu:GDPNP:EF-Ts complex (TTTP)

The crystals of the EF-Tu:GDPNP:EF-Ts complex contained two molecules, A and B, per asymmetric unit. As in TTDPa, two alternate conformations denoted A and B were modeled for GDPNP and the occupancy refined to 0.46 and 0.54 in molecule A for TTTPAA and TTTPAB, respectively. In general, only the α and β-phosphates are fully accommodated in the P-loop and as in TTDPbAB this does not cause a back flip of the carbonyl group of uV20. In TTTPB and one of the alternate conformations in complex A of the asymmetric unit, TTTPAA, the γ-imino group of GDPNP molecule interacts through a hydrogen bond with the carbonyl group of uV20 (Fig. 2D).

Comparison to the EF-Tu:GDPNP structure shows that sufficient space is available to fully accommodate the GDPNP, but this is likely to be energetically unfavorable as the charge of the GDPNP is not compensated by the presence of a Mg^{2+}-ion. As in EF-Tu:EF-Ts and TTP, the side chain of uK24 is pointing towards uD80 and is stabilized by a hydrogen bond, while the electron density of uD21 again suggest a flexible side chain able to form a hydrogen bond with sK51 (Figs. 2D, S2G, and H) In the ribose- and guanine-binding pocket, the interaction between uD138 and guanine is reestablished, however still slightly farther apart than in TTDPa.

3.5. Structure of the EF-Tu:GDPNP:pulvomycin:Mg^{2+}:EF-Ts complex (TTTPuM)

The structure of TTTPuM shows the movement of EF-Tu domain 1 towards its GTP conformation (Figs. 1B, S1 and 3A), and represents the final step in the nucleotide exchange pathway immediately prior to release of EF-Ts.

The structure of EF-Tu is essentially the same as that observed in the complex of EF-Tu:GDPNP:pulvomycin (Parmeggiani et al., 2006) except that the majority of the switch 1 region is disordered in the present structure.

The domain arrangement of EF-Ts has changed to accommodate the conformational transition of EF-Tu to its GTP conformation. EF-Ts remains bound to EF-Tu through interactions of its N-terminal domain and subdomain C with domains 1 and 3 of EF-Tu, respectively. In contrast, the interaction between the conserved TDFV motif of EF-Ts and helices B and C of EF-Tu is abolished. In this novel conformation, the N-terminal and coiled-coil domains of EF-Ts interacts (Fig. 3A and B), whereby, the coiled-coil domain has become displaced by up to 4 Å as compared to the TTDPa structure (Fig. S4). In addition, the orientation of the coiled-coil domain is slightly altered with respect to subdomain C. This displacement of the coiled-coil domain may affect the interface between domain 3 of EF-Tu and subdomain C of EF-Ts (Fig. 3C). The N-terminal domain of EF-Ts additionally contacts domain 3 of EF-Tu at uK313 (Fig. 3D). This residue is conserved in prokaryotic, chloroplast and mitochondrial EF-Tu sequences, but not found in eukaryotic eEF1A, where the corresponding loop is five residues shorter (Fig. S5). The structure of TTTPuM shows uK313 close to sK51 and sK47 close to uR381 (Fig. 3D). These unfavorable interactions thus may destabilize the complex.

In order for this rearrangement of EF-Ts to occur, the C-terminal half of EF-Ts helix 3 connecting the N-terminal domain and subdomain N of EF-Ts unwinds from position sG44 and becomes extended. The "breaking point" at sG44 is conserved as a glycine in more than 90% of known EF-Ts sequences. In the remaining 10% of known EF-Ts sequences, a glycine is found in the subsequent position. In addition, a small movement of the EF-Ts helices 4, 5, 6, and 7 of up to 1.7 Å is observed (Fig. S4). The C-terminal extension of EF-Ts is released from EF-Tu and electron density is seen for the first part of the extension folding back onto subdomain C. Electron density for GDPNP is clearly seen, whereas density is only observed for parts of pulvomycin. The Mg^{2+} ion has been included in the model and is within density although a distinct peak in the electron density cannot be observed at this resolution.

4. Discussion

In this study, the structures of five intermediate complexes formed during the EF-Ts-catalyzed guanine-nucleotide exchange reaction on EF-Tu have been determined at resolutions between 1.84 and 3.5 Å. The most prominent structural change is the rearrangement towards a GTP-like conformation of EF-Tu observed in the TTTPuM structure. In addition, a comparison of the structures determined to better than 2.2 Å resolution identifies a set of interactions important for the nucleotide exchange reaction: uK24 with either uD80 or the phosphates of the nucleotide, sK51 with uD21, uK136 with uD21(mc), uH22 with uD109 and uD138 with the guanine ring of the nucleotide.

The structures presented here along with previously determined structures can be ordered to provide a detailed description of the course of guanine-nucleotide exchange as follows: EF-Tu:GDP:Mg^{2+} (Song et al., 1999), EF-Tu:GDP:Mg^{2+}:EF-Ts (undescribed); EF-Tu:GDP:EF-Ts (TTDPa and b, this study); EF-Tu:PO_4:EF-Ts (TTP, this study); EF-Tu:EF-Ts (Kawashima et al., 1996b); EF-Tu:PO_4:EF-Ts (this study); EF-Tu:GDPNP:EF-Ts (TTTP, this study); EF-Tu:GDPNP:pulvomycin:Mg^{2+}:EF-Ts (TTTPuM, this study); EF-Tu:GDPNP:Mg^{2+} (Kjeldgaard et al., 1993). The course of the individual events is outlined in the following and summarized in Fig. 4. Selected biochemical data for wild-type and mutant forms of EF-Tu and EF-Ts are presented in support of the model.

4.1. Binding of EF-Ts to the EF-Tu:GDP:Mg^{2+} complex

The flexibility within EF-Ts, demonstrated by the TTTPuM structure, suggests that binding at both helix D and domain 3 of EF-Tu is possible without affecting the relative domain orientation in EF-Tu:GDP and hence occurs before the exchange reaction proceeds (Fig. 4, step a). The establishment of stable contacts at both interfaces appears to be required, since the double mutations sM19E/sM20E or sV234E/sM235E located on the EF-Ts side of the interfaces completely destroy overall EF-Ts function (Zhang et al., 1998). Likewise, mutations of residues in EF-Tu interacting with the N-terminal domain of EF-Ts, i.e. L148A and E152A, reduce the rate of initial complex formation (Wieden et al., 2002).

However, the structure of the initial EF-Tu:Mg^{2+}:GDP:EF-Ts complex must be slightly different from any of the structurally characterized complexes to avoid a clash between helix B of EF-Tu and subdomain N of EF-Ts. Thus, adjustment of the interface between subdomain C of EF-Ts and domain 3 of EF-Tu is required, which is probably accompanied by a small movement of helix C of EF-Tu caused by the interaction of sR12 with the carbonyl groups of uD109 and uP111. The importance of sR12 during binding is

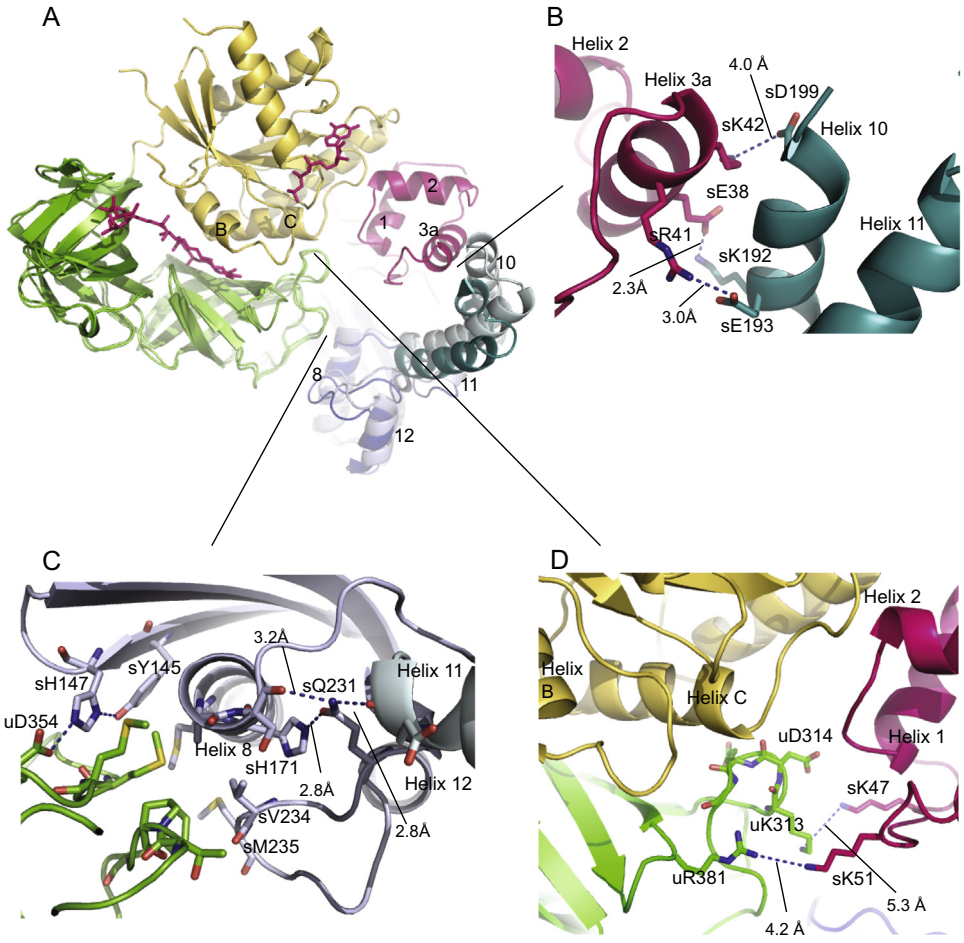

Fig. 3. Structural details related to the TTTPuM structure. (A) Cartoon view of TTTPuM rotated by 90° with respect to the view in Fig. 1, but with the same color coding. TTDP is superimposed using Cα-atom coordinates of EF-Tu domains 2 and 3 to show the movement of the EF-Ts coiled-coil helices 10 and 11. Selected helices are labeled for reference with roman capitals in EF-Tu and numbers in EF-Ts. Lines indicate the positions of the areas highlighted in panels (B), (C) and (D). (B) Contacts between helices 3a and 10 of EF-Ts. (C) Interactions in the TTDPa structure of the conserved sQ231 with EF-Ts helices 11 and 12 forming part of the hydrophobic interface between subdomain C and domain 3 of EF-Tu. (D) Interface between the N-terminal domain of EF-Ts and domains 1 and 3 of EF-Tu showing the proximity between the prokaryotic conserved loop 313–317 and the N-terminal domain of EF-Ts. See also Figs. S4 and S5.

reflected by the severe effect on complex formation observed for the double mutant sK9A/R12A (Zhang et al., 1998).

4.2. Release of the magnesium ion

After initial binding of EF-Ts, EF-Tu is basically still in its GDP conformation. Next, the linker between the N-terminal domain and subdomain N and the interface between subdomain C of EF-Ts and domain 3 of EF-Tu will relax into the conformation observed in TTDP. These changes occur in EF-Ts and cause a separation of EF-Tu domain 1 from domains 2 and 3 thereby providing space for helix B to alter its conformation (Fig. 4, step b). This conformational change is reinforced by subdomain N of EF-Ts pushing back on the N-terminal end of helix B causing a displacement of uD80 away from the Mg^{2+} binding site. Consequently, the Mg^{2+} ion is released and phosphate binding is destabilized.

The movement of helix B is completed by sD80 stabilizing the main chain of uH84 and uA85 and the insertion of sF81 between uH84 and uH118 of helices B and C, respectively. Originally, it was suggested that the sF81 insertion was driving the separation of helix B and C, and it was therefore surprising that the sF81A mutation only had a moderate effect on the overall exchange reaction (Zhang et al., 1996). In our model, the role of sF81 is merely to exclude water for entering the space between helix B and C, so that the movements of helix B and C will not be obstructed by the presence of water. The kinetics of the uH84A mutant reveals the importance of the conformational change in helix B as the increased flexibility introduced by substituting the histidine by an alanine increases the rate of both GDP and GTP release 4 fold (Schummer et al., 2007). Similarly, the uG83A mutation decreasing the flexibility of the DXXG loop causes a decrease in the overall exchange rate (Kjaersgard et al., 1995). The reduction of the rates of nucleotide dissociation observed upon mutation of uH118 (Dahl et al., 2006) is most likely caused by preventing conformational changes in helix C. Furthermore, interactions between sR12 and the main chain of uD109 and uP111 aid in the separation of helices B and C.

4.3. Destabilization and release of bound GDP

The binding of the phosphates is further destabilized by a flip of the amino group of uK24 to form a saltbridge with uD80 as seen in TTDPaB (Figs. 2A and 4, steps c and d). In TTDPa, the interaction of EF-Ts with EF-Tu at helix D has not progressed to a change in the NKXD motif, whereas in TTDPbB, uD138 is retracted slightly from the guanine ring. (Fig. 2B). This destabilization allows the β-phosphate to swing out of the P-loop, while the α-phosphate moves away from the guanine-binding pocket in concert with the flip of the uV20 carbonyl group (Fig. 4, step d). This movement

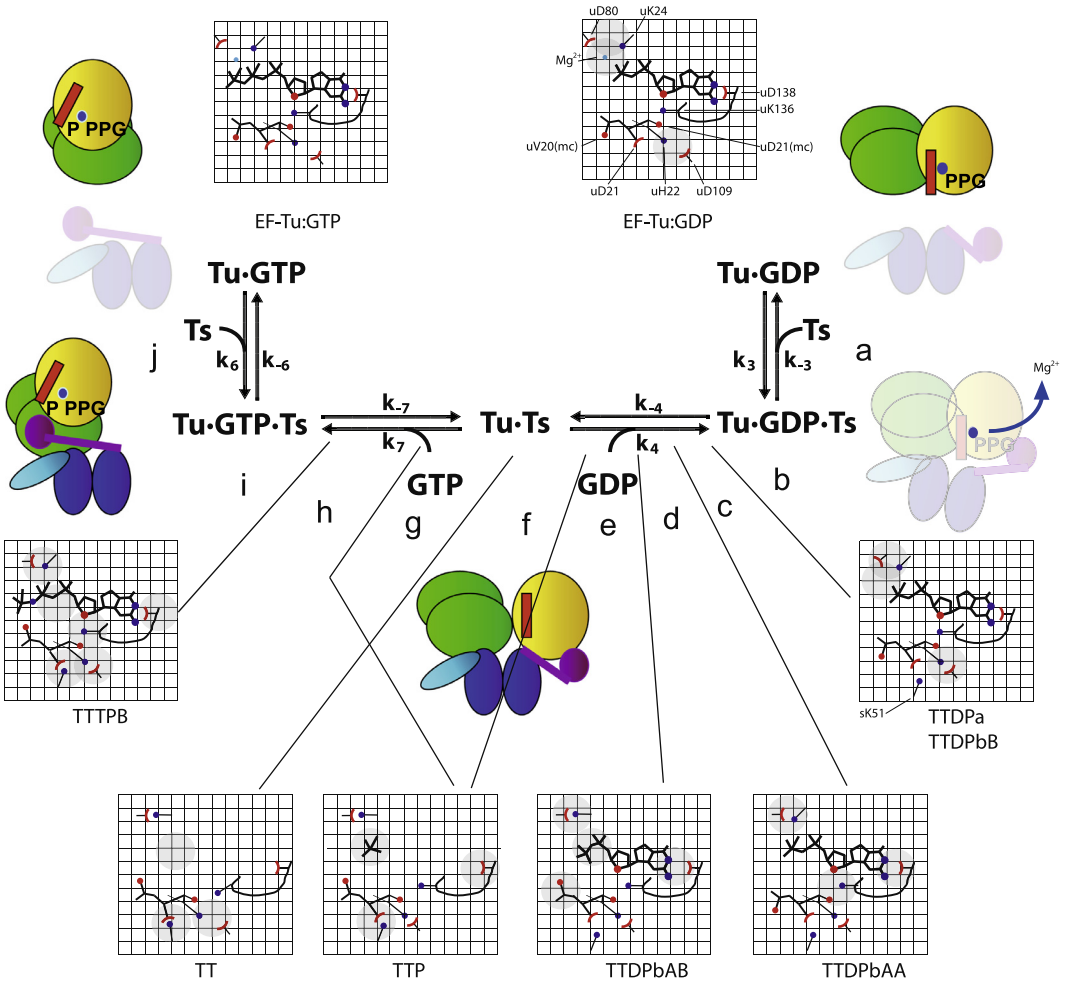

Fig. 4. Schematic representation of the guanine nucleotide exchange reaction. The cartoon models represent the different states in the kinetic model shown in the middle part of the figure. The reaction cycle is labeled with the symbols for rate constants previously used in the literature e.g. (Gromadski et al., 2002). Domains of the elongation factors are shown as elliptic shapes color-coded as in Fig. 1. In addition, helix B is indicated as a red bar, the Mg^{2+}-ion as a blue circle, and the linker region between the N-terminal domain and subdomain N of EF-Ts is shown as a magenta bar. The structures shown as dimmed cartoons have not been determined, i.e. free EF-Ts and the postulated initial complex of EF-Tu:GDP:Mg^{2+}:EF-Ts before release of Mg^{2+}. The steps referred to in the main text are indicated with lower-case letters. Schematic representations of selected interactions in the nucleotide-binding site are shown in small grids in the order they occur along the reaction path. These close-ups correspond to known structures as indicated below each of the grids. The individual elements of these grids are labeled at the top right for the grid representing EF-Tu:GDP except for sK51, which is labeled in the grid representing TTDPa. Interactions changing from one grid to the next are indicated by gray shading and the important release of the Mg^{2+} in step b is indicated by the blue arrow.

of the phosphates is accompanied by increased flexibility of the ribose and guanine ring as observed in TTDPbA and leads to the state prior to release of the α-phosphate (Fig. 4, step e). Thus, the β-phosphate and the ribose/base appear to be released simultaneously.

It has previously been suggested that the decreased rate constant of GDP release observed for the mutations uL148A and uE152A indicated that these affected the NKXD motif and hence supported a base-side-first mechanism of release (Wieden et al., 2002). Since the position of sR12 is stabilized by the salt bridge with uE152 (Fig. S1), our model suggests that the effects of these mutations are rather to interfere with the interaction between sR12 and the main chain of uD109 and uP111 thereby affecting the separation of helices B and C of EF-Tu. The similarities in binding of the guanine ring in EF-Tu:Mg^{2+}:GDP and TTDPa support this.

4.4. Phosphate release and rebinding

The final part of the GDP that needs to be released is the α-phosphate (Fig. 4, step f). This step is accompanied by an opening of the P-loop caused by the closer interaction between uD21 and sK51, the position of which is now stabilized by a hydrogen bond to sQ78. For subsequent accommodation of a new nucleotide, the reverse sequence of events will take place. The initial binding of the α-phosphate of either a GDP or GTP molecule causes a contraction of the P-loop (Fig. 4, step g).

4.5. Binding of GTP

Next, the guanine ring and ribose is accommodated (Fig. 4, step h). The structure of the TTTP complex shows the GDPNP trapped in an otherwise transient state probably both because of the charge of the phosphates, which is not compensated by the presence of the Mg^{2+} and due to the interaction between the uV20 carbonyl group and the γ-imino-group of GDPNP as seen in TTTPB and TTTPAB. If a regular GTP molecule was accommodated in the presence of Mg^{2+}, the uV20 carbonyl group would instead flip causing a movement of uD21 whereby the interaction with sK51 would be destroyed. This state would be similar to TTDPaA except for the presence of the γ-phosphate (Fig. 2A). Step h, being similar to the reverse of step e, is expected to lead to a state similar to TTDPa, where uK24 has moved away from uD80 and points towards the phosphates. The γ-phosphate would now be accommodated and assume a position similar to what is observed in EF-Tu:Mg^{2+}:GDPNP.

Finally, the accommodation of Mg^{2+} is required for the transition to the conformation from which EF-Ts later is released, which is in line with the observation that TTTPuM crystals were obtained only in the presence of Mg^{2+} and crystals of TTTP only in the absence of Mg^{2+}. However, a recent structure of *E. coli* EF-Tu in complex with GDPNP shows that the tri-phosphate and Mg^{2+} can be accommodated without triggering the transition to the compact form of EF-Tu (J.S. Johansen et al., unpublished). A similar phenomenon has been observed for the GTP-bound form of ras p21, which has been shown to exist in a dynamic equilibrium between an active and an inactive conformation (Geyer et al., 1996).

Overall EF-Ts acts by stabilizing intermediates in the exchange reaction facilitating the transition between the active and inactive conformation of EF-Tu. By separating domain 1 from domains 2 and 3 EF-Ts provides space for rearrangements in the switch I and II regions. In addition EF-Ts stabilizes the empty nucleotide-binding site through the salt bridge between uD21 and sK51. This interaction is abolished upon accommodation of the nucleotide and by virtue of the flexible helix connecting the N-terminal domain and subdomain N of EF-Ts the exchange complex persists until the proper EF-Tu nucleotide conformation is reached. As the movement of domain 1 of EF-Tu and the N-terminal domain of EF-Ts occur, sF81 is retracted from its position between helices B and C of EF-Tu (Fig. 4, step i and reverse step b). During this step, helices B and C are moving in agreement with the observed reductions in the rate constants of nucleotide binding for the mutants uH118A and uH118E (Dahl et al., 2006), which are associated with problems of helix C movement.

4.6. Release of the exchange factor

The structure of TTTPuM shows the exchange complex prior to release of EF-Ts from EF-Tu:Mg^{2+}:GTP, an intermediate not previously described structurally for any complex between a G-binding protein and its GEF. Pulvomycin blocks for the complete movement of EF-Tu domain 1 to its GTP conformation and thereby allows the trapping of this intermediate. The binding of pulvomycin to EF-Tu is compatible with the binding of EF-Ts and stabilizes a late intermediate in the nucleotide exchange reaction, where GTP binding is enhanced and GDP binding is reduced (Anborgh et al., 2004).

At this point in the reaction pathway, the nucleotide has been accommodated in its binding pocket, but full binding has not yet been established as the interaction between uT61 of helix A″ and the γ-phosphate is not present. Binding of the guanine ring may also still be incomplete as the destabilizing interaction between the N-terminal domain of EF-Ts and helix D of EF-Tu persists.

We suggest that the release of EF-Ts from EF-Tu:Mg^{2+}:GTP is caused by the continuing movement of domain 1 of EF-Tu towards its GTP conformation whereby destabilizing inter- and intra-molecular interactions will occur (Fig. 4, step j). The proximity of the charges on uK313, sK47 and sK51 will be unfavorable (Fig. 3D). The movement in EF-Tu and the EF-Ts N-terminal domain will in turn alter the position of the coiled-coil domain including its C-terminal part, which is hydrogen bonding sQ231. The effect will propagate to the interface between subdomain C of EF-Ts and domain 3 of EF-Tu as sQ231 is forming a hydrogen bond to sH171 (Fig. 3C).

Thus, EF-Ts will adapt to the nucleotide-binding status of EF-Tu and consequently be released from the EF-Tu:EF-Ts:nucleotide complex in different conformations depending on the identity of the bound nucleotide. More extensive structural rearrangements are required for release of EF-Ts from the EF-Tu:GTP:EF-Ts complex explaining why EF-Ts dissociates 6–7 times faster from the EF-Tu:GDP:EF-Ts complex (Gromadski et al., 2002).

The release of EF-Ts from the EF-Tu:Mg^{2+}:GTP:EF-Ts complex may be further stimulated by the presence of aa-tRNA (Bubunenko et al., 1992; Romero et al., 1985) and a recent pre-steady state kinetic study suggests that simultaneous presence of aa-tRNA and EF-Ts significantly increases the rate of formation of the EF-Tu:GTP:aa-tRNA complex by facilitating rate-limiting structural rearrangements in the nucleotide-binding site (Burnett et al., 2013). The present structures allow a refinement of this interpretation and suggest that the coiled-coil domain of *E. coli* EF-Ts may contribute to capturing aa-tRNA and facilitate proofreading of the charging status of the tRNA (Fig. 5). Several features indicate the possibility of binding tRNA to the EF-Tu:Mg^{2+}:GTP:EF-Ts complex: (1) the length of the tRNA acceptor arm fits the distance from the coiled-coil domain of EF-Ts to the aminoacyl binding site in domain 2 of EF-Tu (Fig. 5A), (2) the coiled-coil motif of EF-Ts resembles the tRNA-binding domain found in several aminoacyl-tRNA synthetases as well as other RNA-binding proteins (Cahuzac et al., 2000) (Fig. 5B), and (3) a distinct basic patch (Fig. 5C) conserved in all prokaryotic EF-Ts sequences (Fig. 5D) is found at the surface of the coiled-coil domain. After the initial capture of the tRNA by EF-Ts, its 3′ end is guided into the aminoacyl binding site of EF-Tu, where the discrimination between charged and uncharged tRNA takes place (Nissen et al., 1996). If the tRNA is aminoacylated, accommodation of aa-tRNA into the ternary complex will proceed with concomitant release of EF-Ts due to steric hindrance between the elbow region of tRNA and residues 237–240 of EF-Ts. In contrast, de-acylated tRNA will not be stabilized by interactions in the EF-Tu binding site and hence dissociate without disruption of the EF-Tu:GTP:EF-Ts complex. Thereby, the amino-acylation state of the tRNA is proofread. Since the residues of EF-Tu responsible for recognition of the amino acyl moiety are all found in domain 2, the interaction between aa-tRNA and EF-Tu:GTP:EF-Ts can occur prior to the conformational change from the open to the closed conformation. Thus, the presence of aa-tRNA leads to an intermediate complex that increases the rate of the conformational transition (Burnett et al., 2014; Burnett et al., 2013).

The potential involvement of the coiled-coil motif of EF-Ts in capturing and guiding tRNA into the aminoacyl-binding pocket of EF-Tu for proofreading of charging is supported by the observation that a mutant strain of *E. coli* with an EF-Ts lacking the coiled-coil domain ceases growth at a lower cell density during amino-acid starvation, which coincides with the point of (p)ppGpp synthesis (Karring et al., 2003). Codon-specific binding of deacylated tRNA to the ribosomal A site triggers the production of (p)ppGpp by the ribosome-associated protein relA giving rise to the socalled stringent response (Haseltine and Block, 1973). In the mutant strain, the proportion of uncharged tRNA delivered to the ribosome is expected to increase due to a less efficient check of charging. This will be particularly pertinent upon starvation and lead to an earlier onset of the stringent response.

4.7. Comparison with other structures of transient G-protein:GEF complexes

Despite the high structural similarity between the guanine-nucleotide binding domains of G-proteins, the corresponding GEFs display no common structural features across classes. Nevertheless, the mechanism of EF-Ts-catalyzed guanine-nucleotide exchange on EF-Tu presented here shares features with the mechanisms of the GEF-catalyzed exchange reaction for small G-proteins (Thomas et al., 2007) and eEF1ABα (Andersen et al., 2001). The general outline of the reaction for small G proteins describes that first the Mg^{2+} ion is released as a result of the GEF action, which leads to either the opening of the binding site through interactions with the switch I and II regions or directly

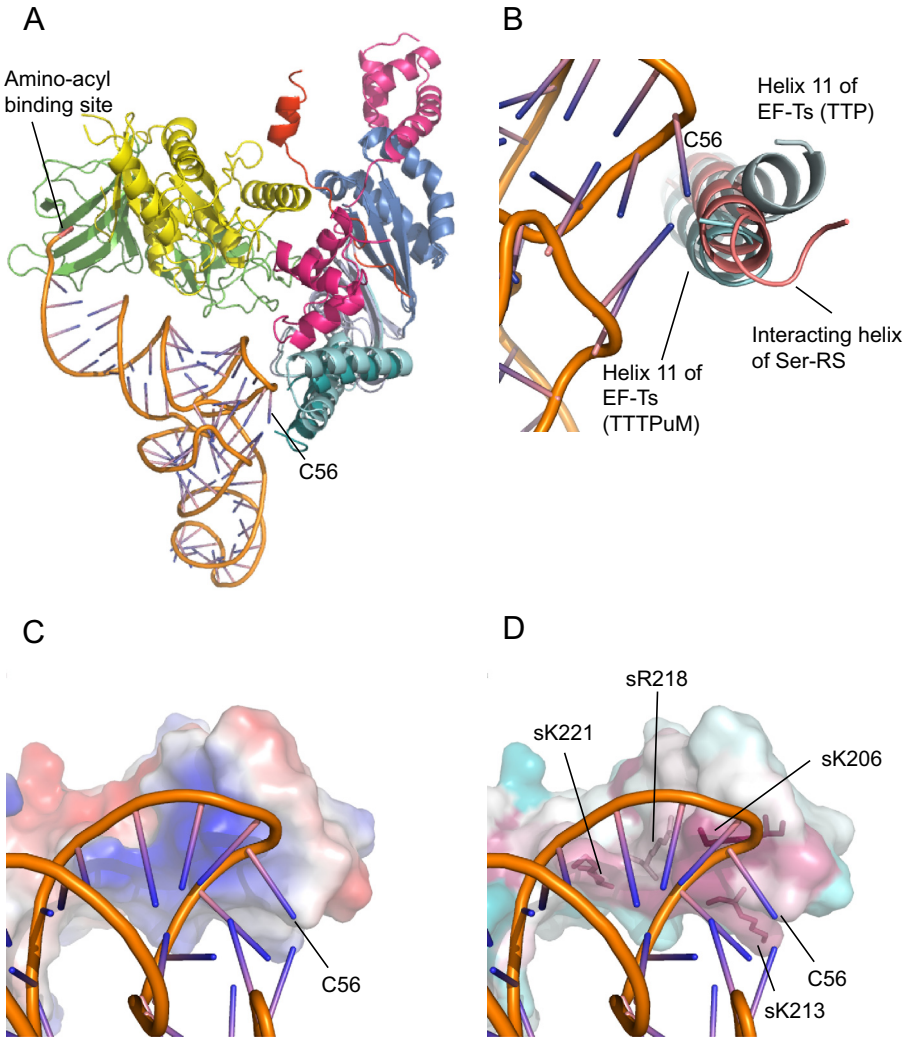

Fig. 5. Potential recognition of aa-tRNA by the EF-Tu:EF-Ts complex. (A) Superposition of TTTPuM and TTDPa using domains 2 and 3 of EF-Tu. Only EF-Tu of TTTPuM is shown. Additionally, Phe-tRNA^{Phe} has been placed with the amino-acyl moiety in the amino-acyl binding-site in domain 2 of EF-Tu and the elbow region close to the EF-Ts coiled-coil domain. The position of tRNA C56 is indicated as a point of reference. (B) Overlay of the helix from seryl-tRNA synthetase interacting with the elbow region of tRNA^{Ser} (PDB:1SER) and helix 11 from TTTPuM and TTDPa. (C) Surface of the coiled-coil domain of TTDPa colored according to electrostatic potential: red – negative; blue – positive. The tRNA is shown in cartoon representation. (D) Surface of the coiled-coil domain of TTDPa colored according to sequence conservation: green – not conserved; red – conserved. The tRNA is shown in cartoon representation.

occludes the Mg^{2+}-binding site. Next, phosphate binding is further destabilized by the formation of the salt bridge between the conserved P-loop lysine and either an acidic residue in the switch II region or an acidic residue provided by the GEF. Thereby, the P-loop lysine is hindered from exerting its stabilizing interaction with the phosphate group. The phosphates are then released and the P-loop either adapts to the absence of the phosphate and/or the P-loop conformation is stabilized by interactions with the GEF. After phosphate release, the rest of the nucleotide dissociates from the G-protein:GEF complex and the conformation of the NKXD-loop adjusts to the absence of the guanine base.

Overall, the mechanism of guanine-nucleotide exchange employed by EF-Ts appears to follow the general mechanism outlined above. Upon binding of EF-Ts to EF-Tu, the switch I region is displaced by the C-terminal helix of EF-Ts. Also the switch II region is moved upon binding due to pushing by subdomain N. Altogether, these changes disrupt the coordination of the Mg^{2+} ion, which dissociates. In contrast to many other G-proteins, there is no obvious intrusion of amino acid residues from the GEF (as seen for e.g. Cdc42:DOCK9 (Yang et al., 2009) or ARA7:VSP9a (Uejima et al., 2010)) or the G-protein itself (as seen for e.g. ROP:PRONE (Thomas et al., 2007)) into the Mg^{2+} binding site. Next, binding of the phosphate moiety of GDP is destabilized by establishment of a salt bridge between uLys24 (from the P-loop) and uAsp80 (from the DXXG motif). A similar mechanism of phosphate destabilization has been observed for ROP:PRONE (Thomas et al., 2007), while in other cases, the GEF inserts one or more residues into the phosphate-binding site (e.g. Arf:Sec7 (Goldberg, 1998)) with the same result that the P-loop lysine is stabilized. At this point in the reaction pathway, the structural changes causing destabilization of phosphate binding propagates from the P-loop to the guanine binding pocket possibly through the lysine of the NKXD motif or direct interaction between the GEF and residues in the vicinity of the NKXD motif. This results in the shift of the α-phosphate position and guanine base. In this way, the release and binding of the base and β/γ-phosphate moieties of the guanine nucleotide may be coordinated, while α-phosphate release/binding is the last/first event during GDP release/GTP binding. This could potentially be a mechanism also employed by other G-GEFs, which would be in agreement with the G-protein:GEF structures

observed with a phosphate or sulfate ion in the P-loop (Buchwald et al., 2002; Guo et al., 2013; Kristelly et al., 2004; Renault et al., 2001; Worthylake et al., 2000). So far, however, EF-Tu is the most prominent example of a G-protein in which a destabilization at the base side appears to play a role during nucleotide exchange.

5. Conclusion

This study has advanced the structural characterization of guanine-nucleotide exchange by providing structures of a number of intermediary states along the reaction pathway of EF-Ts-mediated replacement of GDP with GTP in EF-Tu. Even though similar intermediates have been characterized for other G-proteins, this is the most complete structural study of the process of guanine-nucleotide exchange allowing an ordering of individual steps along the pathway. The structures suggest a novel sequence in nucleotide release as compared to previously studied G-protein:GEF complexes: first a concerted destabilisation of the β-phosphate and base occurs followed by final release of the α-phosphate. Additionally, a unique complex trapped by the antibiotic pulvomycin sheds light on the very last step before release of the GTP-bound form of EF-Tu from EF-Ts. This latter structure also provides a structural framework for suggesting a mechanism of proofreading the charging status of tRNA.

Acknowledgements

We are deeply indebted to Jens Nyborg for initiating the structural studies of translation elongation factors and for his continuous support and encouragement until his death in 2005. We acknowledge economic support from the Danish Council for Independent Research (Natural Sciences).

Appendix A. Supplementary data

Supplementary data associated with this article can be found, in the online version, at http://dx.doi.org/10.1016/j.jsb.2015.06.011.

References

Anborgh, P.H., Okamura, S., Parmeggiani, A., 2004. Effects of the antibiotic pulvomycin on the elongation factor Tu-dependent reactions. Comparison with other antibiotics. Biochemistry 43, 15550–15556.
Andersen, G.R., Valente, L., Pedersen, L., Kinzy, T.G., Nyborg, J., 2001. Crystal structures of nucleotide exchange intermediates in the eEF1A–eEF1Balpha complex. Nat. Struct. Biol. 8, 531–534.
Berchtold, H., Reshetnikova, L., Reiser, C.O.A., Schirmer, N.K., Sprinzl, M., Hilgenfeld, R., 1993. Crystal structure of active elongation factor Tu reveals major domain rearrangements. Nature 365 (126), 132.
Bogestrand, S., Wiborg, O., Thirup, S., Nyborg, J., 1995. Analysis and crystallization of a 25 kDa C-terminal fragment of cloned elongation factor Ts from *Escherichia coli*. FEBS Lett. 368, 49–54.
Bourne, H.R., Sanders, D.A., McCormick, F., 1991. The GTPase superfamily: conserved structure and molecular mechanism. Nature 349, 117–127.
Bubunenko, M.G., Kireeva, M.L., Gudkov, A.T., 1992. Novel data on interactions of elongation factor Ts. Biochimie 74, 419–425.
Buchwald, G., Friebel, A., Galán, J., Hardt, W., Wittinghofer, A., Scheffzek, K., 2002. Structural basis for the reversible activation of a Rho protein by the bacterial toxin SopE. EMBO J. 21, 3286–3295.
Burnett, B.J., Altman, R.B., Ferguson, A., Wasserman, M.R., Zhou, Z., Blanchard, S.C., 2014. Direct evidence of an elongation factor-Tu/Ts.GTP.Aminoacyl-tRNA quaternary complex. J. Biol. Chem. 289, 23917–23927.
Burnett, B.J., Altman, R.B., Ferrao, R., Alejo, J.L., Kaur, N., Kanji, J., Blanchard, S.C., 2013. Elongation factor Ts directly facilitates the formation and disassembly of the *Escherichia coli* elongation factor Tu·GTP·aminoacyl-tRNA ternary complex. J. Biol. Chem. 288, 13917–13928.
Cahuzac, B., Berthonneau, E., Birlirakis, N., Guittet, E., Mirande, M., 2000. A recurrent RNA-binding domain is appended to eukaryotic aminoacyl-tRNA synthetases. EMBO J. 19, 445–452.
Dahl, L.D., Wieden, H.J., Rodnina, M.V., Knudsen, C.R., 2006. The importance of P-loop and domain movements in EF-Tu for guanine nucleotide exchange. J. Biol. Chem. 281, 21139–21146.
Geyer, M., Schweins, T., Herrmann, C., Prisner, T., Wittinghofer, A., Kalbitzer, H.R., 1996. Conformational transitions in p21ras and in its complexes with the effector protein Raf-RBD and the GTPase activating protein GAP. Biochemistry 35, 10308–10320.
Goldberg, J., 1998. Structural basis for activation of ARF GTPase: mechanisms of guanine nucleotide exchange and GTP-myristoyl switching. Cell 95, 237–248.
Gromadski, K.B., Wieden, H.J., Rodnina, M.V., 2002. Kinetic mechanism of elongation factor Ts-catalyzed nucleotide exchange in elongation factor Tu. Biochemistry 41, 162–169.
Guo, Z., Ahmadian, M.R., Goody, R.S., 2005. Guanine nucleotide exchange factors operate by a simple allosteric competitive mechanism. Biochemistry 44, 15423–15429.
Guo, Z., Hou, X., Goody, R.S., Itzen, A., 2013. Intermediates in the guanine nucleotide exchange reaction of Rab8 protein catalyzed by guanine nucleotide exchange factors Rabin8 and GRAB. J. Biol. Chem. 288, 32466–32474.
Haseltine, W.A., Block, R., 1973. Synthesis of guanosine tetra-and pentaphosphate requires the presence of a codon-specific, uncharged transfer ribonucleic acid in the acceptor site of ribosomes. Proc. Natl. Acad. Sci. U. S. A. 70, 1564–1568.
Jeppesen, M.G., Navratil, T., Spremulli, L.L., Nyborg, J., 2005. Crystal structure of the bovine mitochondrial elongation factor Tu.Ts complex. J. Biol. Chem. 280, 5071–5081.
Karring, H., Bjornsson, A., Thirup, S., Clark, B.F., Knudsen, C.R., 2003. Functional effects of deleting the coiled-coil motif in *Escherichia coli* elongation factor Ts. Eur. J. Biochem. 270, 4294–4305.
Kawashima, T., Berthet-Colominas, C., Cusack, S., Leberman, R., 1996a. Interconversion of crystals of the *Escherichia coli* EF-Tu·EF-Ts complex between high- and low-diffraction forms. Acta Crystallogr. D Biol. Crystallogr. 52, 799–805.
Kawashima, T., Berthet-Colominas, C., Wulff, M., Cusack, S., Leberman, R., 1996b. The structure of the *Escherichia coli* EF-Tu:EF-Ts complex at 2.5 Å resolution. Nature 379, 511–518.
Kjaersgard, I.V., Knudsen, C.R., Wiborg, O., 1995. Mutation of the conserved Gly83 and Gly94 in Escherichia coli elongation factor Tu. Indication of structural pivots. Eur. J. Biochem. 228, 184–190.
Kjeldgaard, M., Nissen, P., Thirup, S., Nyborg, J., 1993. The crystal structure of elongation factor EF-Tu from *Thermus aquaticus* in the GTP conformation. Structure 1, 35–50.
Knudsen, C.R., Clark, B.F., Degn, B., Wiborg, O., 1992. One-step purification of *E. coli* elongation factor Tu. Biochem. Int. 28, 353–362.
Kristelly, R., Tao, G., Tesmer, J.J., 2004. Structural determinants of RhoA binding and nucleotide exchange in leukemia-associated Rho guanine-nucleotide exchange factor. J. Biol. Chem. 279, 47352–47362.
Nissen, P., Kjeldgaard, M., Thirup, S., Clark, B.F., Nyborg, J., 1996. The ternary complex of aminoacylated tRNA and EF-Tu-GTP. Recognition of a bond and a fold. Biochimie 78, 921–933.
Nissen, P., Kjeldgaard, M., Thirup, S., Polekhina, G., Reshetnikova, L., Clark, B.F., Nyborg, J., 1995. Crystal structure of the ternary complex of Phe-tRNAPhe, EF-Tu, and a GTP analog. Science 270, 1464–1472.
Parmeggiani, A., Krab, I.M., Okamura, S., Nielsen, R.C., Nyborg, J., Nissen, P., 2006. Structural basis of the action of pulvomycin and GE2270 A on elongation factor Tu. Biochemistry 45, 6846–6857.
Parmeggiani, A., Nissen, P., 2006. Elongation factor Tu-targeted antibiotics: four different structures, two mechanisms of action. FEBS Lett. 580, 4576–4581.
Polekhina, G., Thirup, S., Kjeldgaard, M., Nissen, P., Lippmann, C., Nyborg, J., 1996. Helix unwinding in the effector region of elongation factor EF-Tu-GDP. Structure 4, 1141–1151.
Renault, L., Guibert, B., Cherfils, J., 2003. Structural snapshots of the mechanism and inhibition of a guanine nucleotide exchange factor. Nature 426, 525–530.
Renault, L., Kuhlmann, J., Henkel, A., Wittinghofer, A., 2001. Structural basis for guanine nucleotide exchange on Ran by the regulator of chromosome condensation (RCC1). Cell 105, 245–255.
Romero, G., Chau, V., Biltonen, R.L., 1985. Kinetics and thermodynamics of the interaction of elongation factor Tu with elongation factor Ts, guanine nucleotides, and aminoacyl-tRNA. J. Biol. Chem. 260, 6167–6174.
Schummer, T., Gromadski, K.B., Rodnina, M.V., 2007. Mechanism of EF-Ts-catalyzed guanine nucleotide exchange in EF-Tu: contribution of interactions mediated by Helix B of EF-Tu. Biochemistry 46, 4977–4984.
Song, H., Parsons, M.R., Rowsell, S., Leonard, G., Phillips, S.E., 1999. Crystal structure of intact elongation factor EF-Tu from *Escherichia coli* in GDP conformation at 2.05 A resolution. J. Mol. Biol. 285, 1245–1256.
Thomas, C., Fricke, I., Scrima, A., Berken, A., Wittinghofer, A., 2007. Structural evidence for a common intermediate in small G protein-GEF reactions. Mol. Cell 25, 141–149.
Uejima, T., Ihara, K., Goh, T., Ito, E., Sunada, M., Ueda, T., Nakano, A., Wakatsuki, S., 2010. GDP-bound and nucleotide-free intermediates of the guanine nucleotide exchange in the Rab5.Vps9 system. J. Biol. Chem. 285, 36689–36697.
Wang, Y., Jiang, Y., Meyering-Voss, M., Sprinzl, M., Sigler, P.B., 1997. Crystal structure of the EF-Tu·EF-Ts complex from *Thermus thermophilus*. Nat. Struct. Biol. 4, 650–656.
Wieden, H.J., Gromadski, K., Rodnin, D., Rodnina, M.V., 2002. Mechanism of elongation factor (EF)-Ts-catalyzed nucleotide exchange in EF-Tu. Contribution of contacts at the guanine base. J. Biol. Chem. 277, 6032–6036.

Worthylake, D.K., Rossman, K.L., Sondek, J., 2000. Crystal structure of Rac1 in complex with the guanine nucleotide exchange region of Tiam1. Nature 408, 682–688.

Yang, J., Zhang, Z., Roe, S.M., Marshall, C.J., Barford, D., 2009. Activation of Rho GTPases by DOCK exchange factors is mediated by a nucleotide sensor. Science 325, 1398–1402.

Yoder, M., Torres, C., Corelli, R., Jurnak, F., 1985. Bulk preparation and crystallization of the *Escherichia coli* elongation factor Tu-Ts complex. Anal. Biochem. 150, 243–248.

Zhang, Y., Li, X., Spremulli, L.L., 1996. Role of the conserved aspartate and phenylalanine residues in prokaryotic and mitochondrial elongation factor Ts in guanine nucleotide exchange. FEBS Lett. 391, 330–332.

Zhang, Y., Yu, N.J., Spremulli, L.L., 1998. Mutational analysis of the roles of residues in *Escherichia coli* elongation factor Ts in the interaction with elongation factor Tu. J. Biol. Chem. 273, 4556–4562.